Article

Evaluating Diatomaceous Earth for Long-Term Use in Hydrogen Storage

Omar A. Radwan, Ahmed Al-Yaseri,* John D. Humphrey, Rajesh Theravalappil, and Mahmoud M. Abdelnaby

ACCESS		📊 Metrics & More		📖 Article Recommendations

ABSTRACT: Efficient hydrogen storage is essential for its use as a sustainable energy carrier. Diatomaceous earth, a high-surface-area siliceous geomaterial, shows potential as a physisorption material for hydrogen storage. This study analyzes diatomaceous earth's long-term characteristics when subjected to high-pressure hydrogen injection. The diatomaceous earth was subjected to a hydrogen pressure of 1200 psi for a period of 80 days at room temperature. Neither notable morphological or mineralogical changes were observed. Nevertheless, there was a slight reduction in fine particles and a slight increase in larger particles. The Brunauer−Emmett−Teller (BET) surface area decreased slightly with a significant decrease in pore width. However, the hydrogen adsorption at 77 K temperature was increased significantly (45.5%) after the hydrogen storage test. Moreover, there was a delayed release of molecular water as the temperature increased. These changes suggest that a condensation reaction has occurred involving some of the opal-A silanol groups (Si−O−H), producing molecular water. Bonding through siloxane bridges (Si−O−Si) results in a significant decrease in pore width and increased hydrophobicity (i.e., the interaction between diatomaceous surface and H_2 was increased), thereby enhancing hydrogen adsorption capacity. These findings indicate that diatomaceous earth holds promise as a material for hydrogen storage, with the potential for its hydrogen adsorption capacity to improve over time.

Evaluating diatomaceous earth (DE) for long-term use in hydrogen storage

Opal-A can condense under high gas pressure, converting silanol groups (Si-O-H) into siloxane groups (Si-O-Si) and water. This reduces pore width and increases hydrophobicity, enhancing hydrogen adsorption.
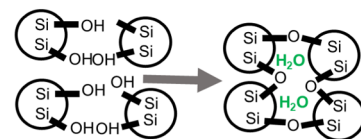
1. INTRODUCTION

Hydrogen is a regenerative and environmentally friendly energy carrier with a very high energy-per-mass ratio.[1] However, hydrogen has a very low energy-per-volume ratio because of its exceptionally low density.[2] Therefore, a huge space is needed for hydrogen storage. Hydrogen storage capacity enhancement approaches are either physical-based or material-based.[3] Physical-based approaches involve the adjustment of physical conditions, including pressure (compressed gas), temperature (liquid), or both (cryo-compressed). In material-based approaches, hydrogen can be stored within the structure (absorption) or on the surface (adsorption) of materials, making it possible to store a large amount of hydrogen in a small volume. Each hydrogen storage method is ideal for some applications (stationary vs mobile, large-scale vs small-scale, and short-term vs seasonal).[4]

Diatoms are unicellular algae that live in almost all kinds of aquatic and semiaquatic environments and secrete silica skeletons (frustules). Diatoms are the most species-rich algae (more than 200 genera and up to 100,000 species). Most species are in the size range of 10−100 μm with pore size in the nanoscale.[5] Diatoms can vary in their surface area, with some species having surface areas as small as a few square meters per gram and others having surface areas as large as several hundred square meters per gram.[6] Vast quantities of diatom frustules can be mined from naturally occurring diatomaceous ooze and diatomite deposits. Diatom frustules can also be produced by cultivating diatoms. Multiple products (including hydrogen, biofuels, fats, fatty acids, polysaccharides, and pigments) can be extracted during culturing diatoms, making the process cost-effective.[7] Diatom species exhibit a wide range of diversity, thriving in both marine and freshwater environments. They display sensitivity to various physical and chemical factors, with each species demonstrating a preference for specific ranges of temperature, salinity, acidity, oxygen levels, and ion concentrations. Manipulation of these parameters can influence diatom productivity.

Diatom-based nanostructures (diatom frustules, diatom replicas, and diatom composites) have been considered for
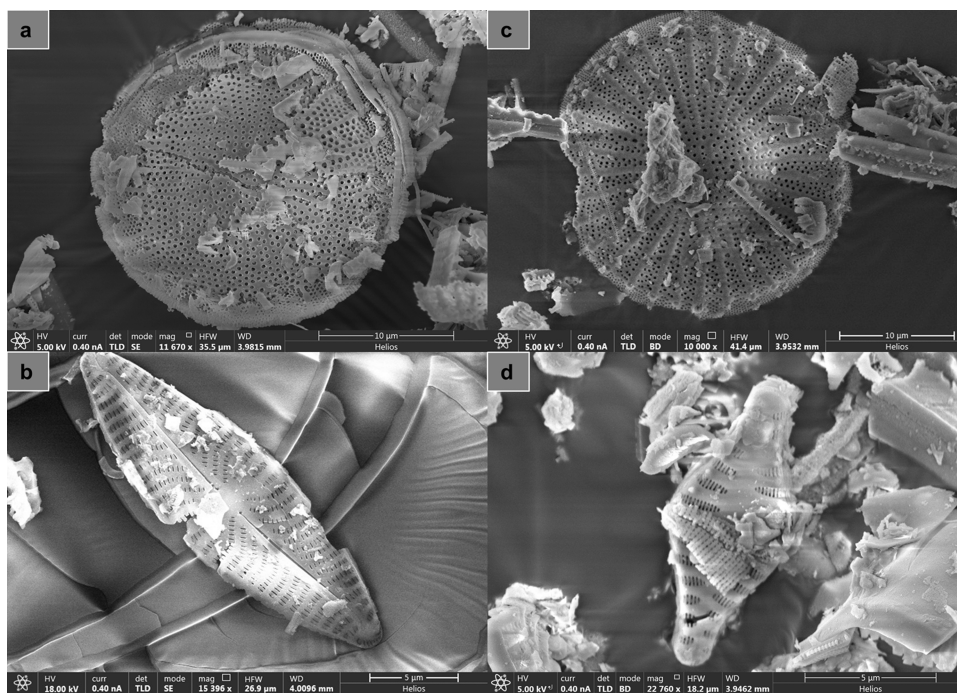
Figure 1. SEM image of diatomaceous earth sample (a, b) before and (c, d) after injecting with hydrogen at 1200 psi for 80 days.

hydrogen storage applications. Diatomaceous earth (DE) has successfully been used as an additive to magnesium hydride (MgH_2), a hydrogen energy storage material, to decrease its desorption temperature. This effect was attributed to its fine porous microstructure.[8] The hydrogen adsorption capacity of DE was found to be high (0.46 wt % at 2.63 MPa and 298 K). Higher values were achieved by acid-thermal activation and noble-metal modification. While the hydrogen adsorption capacity of acid-thermally activated DE reaches 0.83 wt %, metal-modified DE achieves 0.69 wt % in the case of Pt and 0.98 wt % in the case of Pd.[9] The recorded value of platinum-loaded mesoporous silica synthesized from DE is 2.32 wt %.[10] Diatomaceous earth has also been tested to increase the hydrogen storage capacity of palladium−cobalt alloy (Pd_3Co) decorated graphene (~2.7 wt %). The addition of DE has improved to 4.83 wt % (at 2 MPa and 298 K). The enhancement was attributed to increased surface area and pore volume.[11] Similarly, DE enabled chromium-based metal−organic frameworks (1−2 wt % at 77 K and 1 bar) to achieve exceptional adsorptive performance (5.9 wt % at 77 K and 1 bar).[12] Therefore, DE is considered a promising physisorption-based material for hydrogen storage at room temperature.[13]

Under increased pressure and temperature, opal-A, the less stable amorphous form of silica found in diatoms, transforms into more stable silica phases such as opal-CT and quartz. This transformation involves the particles undergoing recrystallization, dehydration, and cementation, leading to their agglomeration and consequent reduction in porosity and surface area.[14,15]

Previous research has yet to investigate the long-term effects of high-pressure hydrogen injection on DE. This study aims to fill this gap by subjecting DE to a 1200 psi hydrogen pressure for 80 days at room temperature to address two primary inquiries: (1) whether storing hydrogen at high pressure in DE induces reactions, recrystallization, cementation, or dehydration; and (2) if such phenomena occur, what consequences

would they have on the surface area and adsorption capability of DE.

2. MATERIALS AND METHODS

A commercial DE sample was placed into a reaction cell to examine the impact of subjecting DE to high-pressure hydrogen over an extended duration. Subsequently, the reaction cell underwent a 30 min vacuuming, followed by the injection of pure hydrogen at a pressure of 1200 psi (82.7 bar). A pressure test was conducted to ensure the absence of any leakage. The cell was then connected to a pressure gauge to provide stable pressure throughout the experiment. Finally, the samples were left undisturbed for 80 days at a pressure of 1200 psi and room temperature. The DE utilized in this study is a natural sample (SA3, Basalt, Nevada) obtained from Dicalite Management Group.

Particle size distribution of the samples was measured before and after the experiment using a laser diffraction particle size analyzer (HELOS/R, Sympatec GmbH) to determine if any agglomeration was occurring. The measurement was performed 3 times using different aliquots.

Thermogravimetric analysis (TGA) was utilized to measure the weight loss percentage of the samples as a function of temperature. Analysis was carried out using a PerkinElmer TGA 8000 system at a rate of 10 °C/min from 25 to 1000 °C in a nitrogen atmosphere. Fourier transform infrared spectroscopy (FTIR) was employed to detect variations in absorption bands corresponding to water molecules and hydroxyl groups before and after the experiment. The analysis was conducted utilizing a Bruker Tensor 27 FTIR spectrometer in transmission mode. X-ray diffraction (XRD) was utilized to identify silica phases and impurities in the samples and to track any phase changes after the experiment. The XRD patterns were recorded using a PANalytical Empyrean diffractometer functioning at 45 kV and 40 mA, using Cu Kα radiation. Samples were scanned 3 times from 4 to 70° 2θ at 0.01° 2θ increments, with 40 s counting time per increment. The

analysis of powder diffraction patterns was performed with Match software, which allowed the identification of phases through the use of the Crystallography Open Database.

To track any morphologic changes after the experiment, a scanning electron microscope (SEM, FEI Helios Nanolab G3 UC) was used.

Surface area measurements were conducted using a surface area analyzer (ASAP2020, Micromeritics) at 77 K through nitrogen sorption isotherm experiments. Before the analysis, the sample was subjected to degassing at 220 °C for 80 min. The Brunauer−Emmett−Teller (BET) technique was employed to ascertain the precise surface area, and the Barrett−Joyner−Halenda (BJH) method was utilized to compute the distributions of pore sizes.

Hydrogen sorption isotherms were measured on an Autosorb IQ (Quantachrome instruments) at 77 K. Prior to the sorption measurements, the samples were activated at 150 °C.

3. RESULTS

Figure 1 shows the SEM photomicrograph of the DE sample before and after the experiment. The sample contains a mixture of centric (Figure 1a−c) and pennate (Figure 1b−d) diatoms. No apparent morphological changes are observed in the structure or pores of diatom frustules after the experiment.

Figure 2a shows the particle distribution density and cumulative distribution density of the DE sample before and after the experiment. Particle sizes (in μm) at 10, 50, and 90% in the cumulative size distribution, denoted as D10, D50, and D90, respectively, are also provided in Table 1. Following the experiment, slight alterations were observed in the D50 and D90 values of the sample. The D10 and D50 values decreased by 10.1, and 3.2%, respectively, while the D90 value showed a 3.3% increase.

Figure 2b shows the thermogravimetric analyses of the DE sample before and after the experiment. At temperatures ranging from room temperature to about 120 °C, both samples show a consistent initial sharp decrease in weight of 3%. Between 110 and 210 °C, the treated sample experiences a higher weight loss of 2.5% compared to the untreated sample, which only loses 1.5%. From 210 to 800 °C, both samples exhibit a gradual weight loss of 2%.

Figure 3a shows the FTIR spectra of the DE sample before and after the experiment. In both samples, two primary absorption bands are evident within the wavenumber range of 1200−4000 cm^{-1}. Notably, the band within the spectral range of 3000−3700 cm^{-1} exhibits reduced prominence after the experiment. Similarly, the intensity of the band around 1630 cm^{-1} is diminished following the experiment.

Figure 3b displays the X-ray diffractogram of the DE sample before and after the experiment. The primary component of the DE sample is opal-A, as shown by the single diffuse reflection at approximately 4.1 Å (~22° 2θ). Both samples contain small amounts of impurities, including quartz, opal-CT, plagioclase, k-feldspar, and clays. Following the experiment, no substantial changes were detected, including increases, decreases, or any notable appearance or disappearance of phases.

Figure 4a shows the nitrogen adsorption−desorption isotherm and the corresponding BJH pore size distributions of the DE before and after the experiment. The isotherm exhibits an H3-type hysteresis loop between relative pressures of 0.4−1.0. This hysteresis loop does not have an adsorption
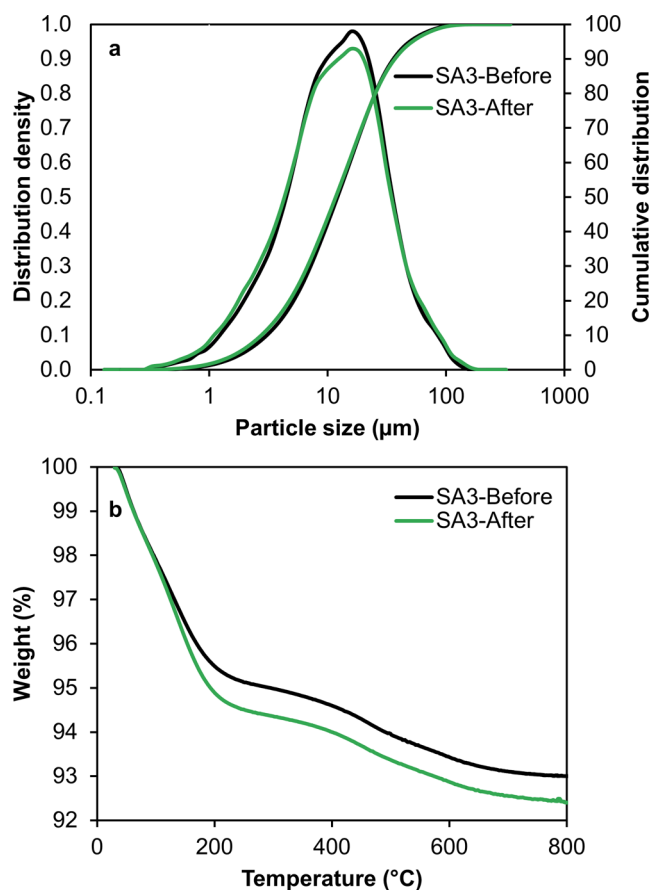

Figure 2. (a) Particle size distribution of diatomaceous earth sample before and after injecting with hydrogen at 1200 psi for 80 days. (b) Thermogravimetric curves of diatomaceous earth sample before and after injecting with hydrogen at 1200 psi for 80 days.

Table 1. Summary of Results

	SA3−before	SA3−after	% change
D10	3.06 ± 0.1	2.75 ± 0.1	10.1% decrease
D50	12.1 ± 0.1	11.7 ± 0.4	3.2% decrease
D90	36.1 ± 0.6	37.3 ± 3.9	3.3% increase
BET surface area (m^2/g)	30.6 ± 0.6	28.9 ± 0.3	5.5% decrease
t-plot micropore area (m^2/g)	10.9	5.3	51.2% decrease
BJH adsorption cumulative volume of pores (cm^3/g)	0.094	0.089	5.3% decrease
BJH desorption cumulative volume of pores (cm^3/g)	0.095	0.085	10.5% decrease
BJH adsorption average pore width (4 V/A) (nm)	19	12.1	36.3% decrease
BJH desorption average pore width (4 V/A) (nm)	18.3	13.2	27.9% decrease
N_2-quantity adsorbed (cm^3/g STP)	64.1	56.1	12.5% decrease
H_2-quantity adsorbed (cm^3/g STP)	3.3	4.8	45.5% increase
weight loss %	6.8 ± 0.02	7.6 ± 0.02	11.1% increase

plateau at high relative pressure (Figure 4a). A distinct spike is seen in the distribution of pore sizes, with the highest concentration occurring in the mesopores range between 3.5−
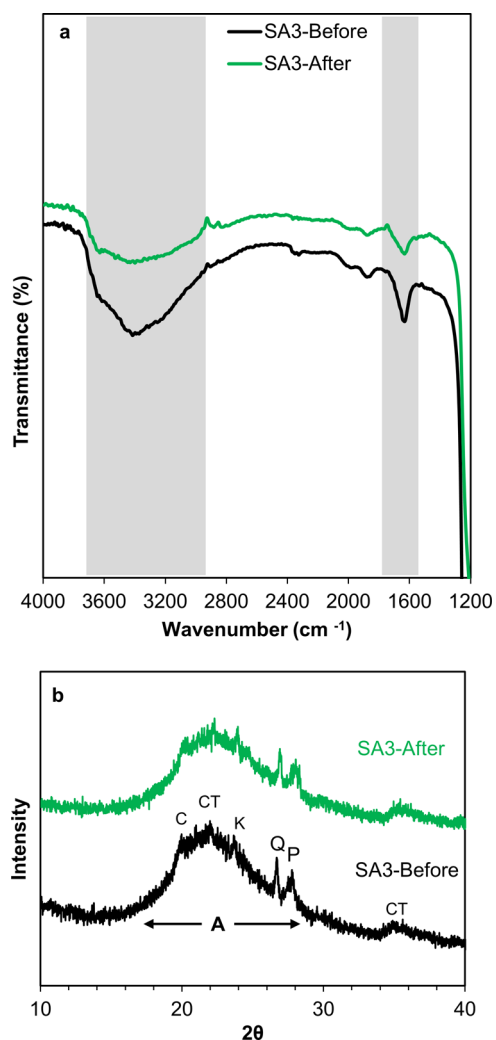
Figure 3. (a) Fourier transform infrared spectroscopy spectra of diatomaceous earth sample before and after injecting with hydrogen at 1200 psi for 80 days. (b) X-ray diffraction pattern of diatomaceous earth sample before and after injecting with hydrogen at 1200 psi for 80 days. A: opal-A, Q: quartz, CT: opal-CT, K: K-feldspar, P: plagioclases, and C: clays.

Figure 4. (a) Nitrogen adsorption−desorption isotherms of diatomaceous earth sample before and after injecting with hydrogen at 1200 psi for 80 days. (b) Pore size distribution. (c) Hydrogen adsorption−desorption isotherms.

4.5 nm (Figure 4b). After the experiment, the DE's specific BET surface area decreased by approximately 5% (Table 1). Similarly, BJH Adsorption and desorption cumulative volume of pores (cm^3/g) exhibited a reduction of approximately 5 and 10%, respectively (Table 1). Notably, the average pore width for BJH adsorption and desorption experienced a more substantial decrease, with reductions of 36.3 and 27.9%, respectively (Table 1). A significant reduction of 51.2% in the *t*-plot micropore area was observed (Table 1). Figure 4c displays the hydrogen adsorption−desorption isotherm of the DE before and after the experiment. The amount of hydrogen adsorbed increased from 3.3 to 4.8, achieving a significant 45.5% increase.

4. DISCUSSION

The SEM results (Figure 1) reveal no notable deterioration and agglomeration of the diatom frustules. Additionally, there is no apparent alteration in the sizes and shapes of the macropores.
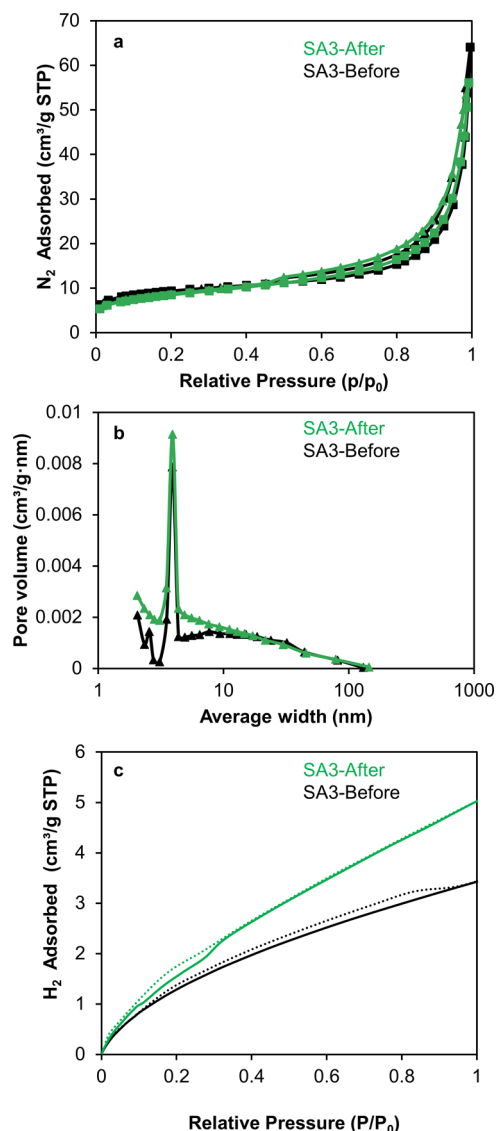
Similarly, the XRD results (Figure 3b) reveal no notable phase changes, which suggests that there is no reactivity with hydrogen. This, in turn, implies that there is no danger of hydrogen loss resulting from any reaction with DE.

The primary component of the DE sample, as shown by the XRD pattern, is opal-A, which is a hydrated amorphous silica phase (Figure 3b). The water present in this opaline silica consists of silanols (OH groups attached to silicon) and molecular water.[16] The TGA analysis reveals two distinct phases of weight reduction (Figure 2b). The initial substantial weight decrease is associated with the elimination of adsorbed molecular water, occurring from room temperature up to 220 °C. This weight loss is more pronounced in the treated sample. Subsequently, there is a gradual reduction in weight, corresponding to the release of water due to the dehydroxylation of silanol groups.

The FTIR examination indicates a noticeable decrease occurring after the experiment in the two bands associated with water molecules and hydroxyl groups (Figure 3a).[17,18]

Specifically, around 3400 cm^{-1}, there is a reduction in the stretching vibration of the O−H bond in both water molecules and silanol groups (Si−OH). Additionally, at approximately 1630 cm^{-1}, there is a decrease in the bending vibration of the H−O−H bond in water molecules.

The nitrogen adsorption−desorption isotherm (Figure 4a) shows an H3-type hysteresis loop, suggesting the presence of macropores in the samples. This is further supported by the SEM image (Figure 1), which confirms the presence of macropores. The BJH pore size distributions (Figure 4b) also indicate the existence of mesopores in the samples, both before and after the experiment. There was a minor reduction in the BET surface area, accompanied by a substantial decrease in the *t*-plot micropore area (Table 1). A discussion of these observations will be provided in the subsequent paragraphs.

We suggest that a condensation reaction has been initiated involving part of the silanol groups, leading to the generation of molecular water (Figure 5). When subjected to high
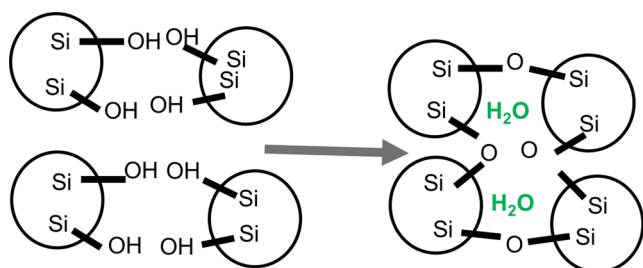

Figure 5. Proposed model of the structure of a diatomaceous earth (DE) sample before and after injecting with hydrogen at 1200 psi for 80 days. DE particles become interconnected by siloxane bridges, leading to the creation of enclosed pores containing trapped water.

pressure, the proximity of silanol groups (Si−O−H) is facilitated by a decrease in available space, leading to the formation of siloxane groups (Si−O−Si) and water molecules (H$_2$O). As a result of the bonding through siloxane bridges, the surface area decreases, and closed pores filled with molecular water are formed. This scenario is founded on the following observations.

1. The decrease in the BET surface area from 30.6 to 28.9 m^2/g indicates the formation of new bonds resulting in reduced surface area. This effect is clearly amplified in the t-plot micropore area and the BJH average pore width. Specifically, the micropore area reduced from 10.9 to 5.3 m^2/g, and the pore width decreased from 19 to 12.1 nm.

2. The increased weight loss observed in the treated sample at temperatures ranging from 110 to 210 °C suggests that the closed pores may have been fractured, leading to the liberation of trapped water. Additionally, it could suggest an increased condensation process involving the remaining silanol groups, which is more favorable in compacted powders compared to noncompacted ones.

3. The reduction observed in the FTIR bands indicates a decrease in both hydroxyl groups and water molecules. This implies a reduction in silanol groups, likely due to their transformation into siloxane groups through a condensation reaction. Furthermore, the decrease in the intensity of the water molecule band can be linked to a decrease in adsorbed water, which in turn is likely influenced by the decrease in surface area.

4. Following the experiment, smaller particle sizes (D10 and D50) decreased slightly, while larger particle sizes (D90) increased slightly. This suggests that a small percentage of fine particles may have agglomerated through condensation, forming larger particles.

A similar response was observed when silica gel, a synthetic hydrous amorphous silica, was subjected to high pressure. Costa et al. compacted silica gel under a hydrostatic pressure of 4.5 GPa at room temperature.[19] The compaction resulted in a decrease in the surface area and a delay in the release of water from the samples, indicating the retention of free water in closed pores. Only when these closed pores ruptured due to the internal pressure of water vapor at higher temperatures was the adsorbed water completely eliminated. This suggests the presence of a strong closed pore structure formed during the high-pressure treatment. The size and strength of these pores can vary, resulting in a temperature range required to eliminate trapped water.

Our conclusion is that the decrease in the surface area of DE, especially in the micropore area, is primarily attributable to the pressure rather than the presence of hydrogen gas. Consequently, we anticipate similar behavior regardless of the gas employed.

Despite a decrease in the surface area, there was a substantial increase in the amount of hydrogen adsorbed. Similar observations were made by Jin et al., who noted that, following an acid-thermal activation treatment, despite a reduction in the surface area of DE, there was an enhancement in hydrogen uptake percentage. They attributed this phenomenon to the shrinkage of pore diameter resulting from acid-thermal activation, which proved beneficial for improving hydrogen adsorption capacity.[9] In our study, a significant reduction in pore width induced by high gas pressure could have led to a similar enhancement in hydrogen adsorption. Another plausible explanation involves the surface dehydroxylation of amorphous silica and the formation of siloxane bridges, promoting hydrophobicity.[20] Previous research has indicated that a hydrophobic silica surface enhances the adsorption of nonpolar gases.[21,22]

5. RECOMMENDATIONS

Figure 6 illustrates a comparison between the literature BET surface area values of diatomite and common natural and synthetic materials typically used for hydrogen storage. Porous
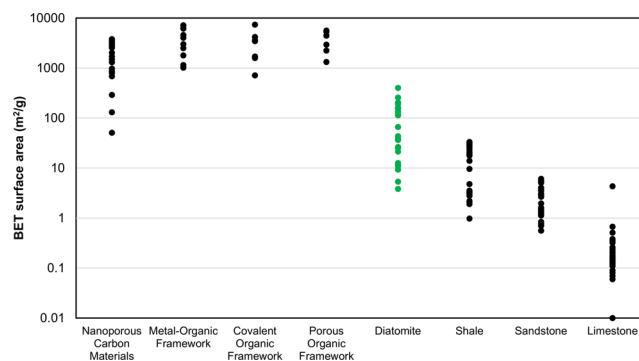

Figure 6. Dot plot comparing the surface area of diatomite with that of various other natural and synthetic materials commonly employed for storing hydrogen. Detailed data can be found in the data availability section.

and permeable formations, suitable for long-term, large-scale underground hydrogen storage, have surface areas significantly lower than diatomite, sometimes by orders of magnitude. Conversely, advanced high-surface-area engineered materials are under development for small-scale onboard automotive hydrogen storage systems. Their surface areas typically range from hundreds to thousands of square meters per gram.

Considering diatomite's affordability and its intermediate position in surface area characteristics between synthetic and other natural materials, it represents a practical option for intermediate-scale hydrogen storage applications like underground tanks for hydrogen fuel stations. Typically, diatomite displays surface areas spanning tens to hundreds of square meters per gram. According to data from the National Minerals Information Center of the U.S. Geological Survey, the average price of DE was $430 per metric ton in 2022.[23]

If DE were to be utilized for hydrogen storage, we recommend the following.

- Selecting diatom species carefully. Diatoms have species-specific surface areas, which can vary significantly. Some diatoms have a surface area of only a few square meters per gram (e.g., *Thalassiosira eccentrica*), while others can have several hundreds of square meters per gram (e.g., *Thalassiosira descipiens*).[6]

- If a species with an extensive surface area is not readily abundant for large-scale mining, diatom cultivation can serve as a viable source substitute.

- Various methods can be employed to enhance the surface area and gas adsorption capabilities of the raw DE. These methods include acid treatment,[24] base treatment,[25] milling,[26] and hydrothermal activation using functional groups.[27]

6. CONCLUSIONS

This study examined the long-term effects of high-pressure hydrogen injection on DE. The results showed that there were no significant changes in the morphology or mineralogy of the DE. However, there was a slight decrease in the size of fine particles and a slight increase in the size of larger particles. The FTIR silanol absorption band, the BET surface area, and BJH pore volume also experienced a slight decrease. Additionally, there was a higher weight loss in the temperature range of 110−210 °C and a significant decrease in *t*-plot micropores.

These findings suggest that the main component of DE, opal-A, may undergo a condensation reaction under high gas pressure. Under elevated pressure conditions, silanol groups (Si−O−H) draw closer and react to form siloxane groups (Si−O−Si) and water molecules (H_2O). This leads to a significant reduction in pore width and an increase in hydrophobicity, which is beneficial for enhancing hydrogen adsorption. Furthermore, we believe that due to diatomite's affordability and its intermediary position in terms of surface area characteristics, situated between synthetic and other natural materials, it represents a practical choice for intermediate-scale hydrogen storage applications, such as underground tanks for hydrogen fuel stations.

ASSOCIATED CONTENT

Data Availability Statement

Data related to this article have been made available at https://zenodo.org/records/10809100.

AUTHOR INFORMATION

Corresponding Author

Ahmed Al-Yaseri − *Center of Integrative Petroleum Research (CIPR), College of Petroleum Engineering and Geoscience, King Fahd University of Petroleum and Minerals, Dhahran 31261, Saudi Arabia*; Email: ahmed.yaseri@kfupm.edu.sa

Authors

Omar A. Radwan − *Geosciences Department, College of Petroleum Engineering & Geosciences (CPG), King Fahd University of Petroleum & Minerals (KFUPM), Dhahran 31261, Saudi Arabia*

John D. Humphrey − *Geosciences Department, College of Petroleum Engineering & Geosciences (CPG), King Fahd University of Petroleum & Minerals (KFUPM), Dhahran 31261, Saudi Arabia*

Rajesh Theravalappil − *Interdisciplinary Research Center for Refining and Advanced Chemicals (IRC-RAC), King Fahd University of Petroleum and Minerals, Dhahran 31261, Saudi Arabia*

Mahmoud M. Abdelnaby − *Interdisciplinary Research Center for Hydrogen Technologies and Carbon Management (IRC-HTCM), King Fahd University of Petroleum & Minerals, Dhahran 31261, Saudi Arabia*

Complete contact information is available at:
https://pubs.acs.org/10.1021/acsomega.4c02415

Notes

The authors declare no competing financial interest.

REFERENCES

(1) Kar, S. K.; Harichandan, S.; Roy, B. Bibliometric Analysis of the Research on Hydrogen Economy: An Analysis of Current Findings and Roadmap Ahead. *Int. J. Hydrogen Energy* 2022, *47* (20), 10803−10824.

(2) Tarhan, C.; Çil, M. A. A Study on Hydrogen, the Clean Energy of the Future: Hydrogen Storage Methods. *J. Energy Storage* 2021, *40*, No. 102676.

(3) Hassan, I. A.; Ramadan, H. S.; Saleh, M. A.; Hissel, D. Hydrogen Storage Technologies for Stationary and Mobile Applications: Review, Analysis and Perspectives. *Renewable Sustainable Energy Rev.* 2021, *149*, No. 111311.

(4) Amirthan, T.; Perera, M. S. A. The Role of Storage Systems in Hydrogen Economy: A Review. *J. Nat. Gas Sci. Eng.* 2022, *108*, No. 104843.

(5) Armstrong, H. A.; Brasier, M. D. Diatoms. In *Microfossils*, 2nd ed.; John Wiley & Sons, Ltd, 2004.

(6) Townley, H. E. Diatom Frustules: Physical, Optical, and Biotechnological Applications. In *The Diatom World*; Seckbach, J.; Kociolek, P., Eds.; Springer : Netherlands Dordrecht, 2011; pp 273−289.

(7) Rai, A.; Khan, M. J.; Ahirwar, A.; Deka, R.; Singh, N.; Schoefs, B.; Marchand, J.; Varjani, S.; Vinayak, V. Hydrogen Economy and Storage by Nanoporous Microalgae Diatom: Special Emphasis on Designing Photobioreactors. *Int. J. Hydrogen Energy* 2022, *47*, 42099−42121, DOI: 10.1016/j.ijhydene.2022.01.057.

(8) Milovanovic, S.; Matović, L.; Drvendžija, M.; Novaković, J. G. Hydrogen Storage Properties of MgH2-Diatomite Composites Obtained by High-Energy Ball Milling. *J. Microsc.* **2008**, *232* (3), 522−525.

(9) Jin, J.; Zheng, C.; Yang, H. Natural Diatomite Modified as Novel Hydrogen Storage Material. *Funct. Mater. Lett.* **2014**, *07* (03), No. 1450027.

(10) Jin, J.; Ouyang, J.; Yang, H. One-Step Synthesis of Highly Ordered Pt/MCM-41 from Natural Diatomite and the Superior Capacity in Hydrogen Storage. *Appl. Clay Sci.* **2014**, *99*, 246−253.

(11) Samantaray, S. S.; Sangeetha, V.; Abinaya, S.; Ramaprabhu, S. Diatom Frustule-Graphene Based Nanomaterial for Room Temperature Hydrogen Storage. *Int. J. Hydrogen Energy* **2020**, *45* (1), 764−773.

(12) Wang, G.; Graham, E.; Zheng, S.; Zhu, J.; Zhu, R.; He, H.; Sun, Z.; Mackinnon, I. D. R.; Xi, Y. Diatomite-Metal-Organic Framework Composite with Hierarchical Pore Structures for Adsorption/ Desorption of Hydrogen, Carbon Dioxide and Water Vapor. *Materials* **2020**, *13* (21), No. 4700, DOI: 10.3390/ma13214700.

(13) Sun, X. W.; Zhang, Y. X.; Losic, D. Diatom Silica, an Emerging Biomaterial for Energy Conversion and Storage. *J. Mater. Chem. A* **2017**, *5* (19), 8847−8859.

(14) Siever, R. Silica Solubility, 0°−200° C., and the Diagenesis of Siliceous Sediments. *J. Geol.* **1962**, *70*, 127−150, DOI: 10.1086/626804.

(15) Isaacs, C. M. *Diagenesis in the Monterey Formation Examined Laterally along the Coast near Santa Barbara*; U.S. Geological Survey: CA; 1980.

(16) Day, R.; Jones, B. Variations in Water Content in Opal-A and Opal-CT from Geyser Discharge Aprons. *J. Sediment. Res.* **2008**, *78* (4), 301−315.

(17) Mohanan, S.; Guan, X.; Liang, M.; Karakoti, A.; Vinu, A. Stimuli-Responsive Silica Silanol Conjugates: Strategic Nanoarchitectonics in Targeted Drug Delivery. *Small* **2023**, No. 2301113, DOI: 10.1002/smll.202301113.

(18) Ellerbrock, R.; Stein, M.; Schaller, J. Comparing Amorphous Silica, Short-Range-Ordered Silicates and Silicic Acid Species by FTIR. *Sci. Rep.* **2022**, *12* (1), No. 11708.

(19) Costa, T. M. H.; Gallas, M. R.; Benvenutti, E. V.; da Jornada, J. A. H. Infrared and Thermogravimetric Study of High Pressure Consolidation in Alkoxide Silica Gel Powders. *J. Non-Cryst. Solids* **1997**, *220* (2), 195−201.

(20) Bolis, V.; Fubini, B.; Marchese, L.; Martra, G.; Costa, D. Hydrophilic and Hydrophobic Sites on Dehydrated Crystalline and Amorphous Silicas. *J. Chem. Soc. Faraday Trans.* **1991**, *87* (3), 497−505.

(21) Al-Yaseri, A.; Esteban, L.; Giwelli, A.; Abdel-Azeim, S.; Sarout, J.; Sarmadivaleh, M. Impact of Wettability on Storage and Recovery of Hydrogen Gas in the Lesueur Sandstone Formation (Southwest Hub Project, Western Australia). *Int. J. Hydrogen Energy* **2023**, *48* (61), 23581−23593.

(22) Day, C.; Barua, N.; Hutter, T. Porous Silica Preconcentrator for Selective Ambient Volatile Organic Compounds Detection: Effects of Surface Functionalization and Humidity. *Appl. Phys. Rev.* **2023**, *10* (2), No. 021401, DOI: 10.1063/5.0139042.

(23) *Mineral Commodity Summaries*; National Minerals Information Center: 2023.

(24) Goren, R.; Baykara, T.; Marsoglu, M. Effects of Purification and Heat Treatment on Pore Structure and Composition of Diatomite. *Br. Ceram. Trans.* **2002**, *101* (4), 177−180.

(25) Tsai, W.-T.; Hsien, K.-J.; Lai, C.-W. Chemical Activation of Spent Diatomaceous Earth by Alkaline Etching in the Preparation of Mesoporous Adsorbents. *Ind. Eng. Chem. Res.* **2004**, *43* (23), 7513−7520.

(26) Hu, Z.; Zheng, S.; Li, J.; Zhang, S.; Liu, M.; Wang, Z.; Li, J.; Sun, H. Pore Structure and Surface Properties of Diatomite with Mechanical Grinding and Its Influence on Humidity Control. *Physicochem. Probl. Miner. Process.* **2022**, *58* (6), No. 153509, DOI: 10.37190/ppmp/153509.

(27) Ren, Z.; He, Y.; Zheng, R.; Guo, Z.; Gao, H.; He, X.; Wu, F.; Ji, X. The Preparation and Characterization of Calcined Diatomite with High Adsorption Properties by CaO Hydrothermal Activation. *Colloids Surf., A* **2022**, *636*, No. 128134.